Modeling of Risley prisms devices for exact scan patterns

Alexandru Schitea, Marius Tuef, Virgil-Florin Duma*
3OM Optomechatronics Group, Aurel Vlaicu University of Arad, 77 Revolutiei Ave., 310130 Arad, Romania

ABSTRACT

We investigate the scan patterns produced using different pairs of Risley prisms. Combinations of optical wedges with different prism angles (corresponding to different deviations angles of the prisms) are considered to complete the exact modeling of the scanning process using specialized mechanical design programs. While this procedure is somehow elaborate with regard to approximate methods, it has the advantage of providing the exact movement laws of the laser spot on various types of surfaces scanned with this type of refractive device. The study is made with regard to the characteristic parameters of the device, such as θ_1 and θ_2 - the prism angles of the two wedges, ω_1 and ω_2 – the rotating speeds of the two wedges, and the geometry of the scanner (which includes the distance between the two prisms, their orientation, and the distance to the scanned plane). The scanner is approached for a row of values of the characteristic parameters $k=\theta_2/\theta_1$ and $M=\omega_2/\omega_1$ introduced in Marshall's classical work. The results allow for choosing the most appropriate patterns for specific scanning applications.

Keywords: optomechanics, optical devices, scanners, Risley prisms, wedges, modeling, scan patterns.

1. INTRODUCTION

Optical and laser scanners [1] have been developed over time in approximately forty different designs [2], uni- (1-D), bi- (2-D), and tri-dimensional (3-D). Out of these numerous designs, the most important ones are [3]: *polygonal* (prismatic and pyramidal) [4, 5], *oscillatory* (galvanometric [6] and resonant – the latter with fixed frequencies, developed especially as MEMS (Micro-Electrical-Mechanical Systems) [7]), *refractive* (with prisms or lenses), *holographic*, as well as *electro-* and *acousto-optical*.

We have approached previously [8] rotating (monogon [9] or polygonal [10]), as well as galvanometer-based scanners (GSs) [11], both for industrial [9] and biomedical imaging applications, the latter with a focus on Optical Coherence Tomography (OCT) [12-14], for which we have demonstrated the optimal scanning regimes of a galvoscanner [15]. In the present study we are approaching the refractive scanner – with rotating Risley prisms / optical wedges.

The applications of this type of scanners range from micro-devices, by example for endoscope probes [16] – with micro-prisms – to devices for satellite positioning – with large prisms for which optomechanical issues become essential [17]. Their domains of application include: Confocal Microscopy (CM) [18], holography [19], interferometry [20, 21], polarimetry [22], beam shaping [23], spectroscopy [24], and optical attenuators. We have developed for the latter a device with translational prisms [25] as an alternative to optical attenuators using optical choppers [26-28]. Combinations of GSs and Risley prisms were also developed for 3-D scanning.

Scanners with Risley prisms have been approached in early works [31], rigorous analitycal analysis were developed [32, 33], and the inverse problem – of determining the positions of the prisms that produce a certain position of the laser spot was approached as well [34]. Constructive solutions were developed for rotational prisms [35], while other devices, by example with titling [36] or with combinations of tilting and rotational wedges were also tested [37].

The scope of our present study is to determine and to analyse the exact scan patterns produced by the classical two Risley prism device. Approximate scan patterns have been determined by Marshall in [38] as Lissajoux figures – using the deviation $D_i=(n-1)\theta_i$, i=1,2 of an optical wedge (where θ_1, θ_2 are the prism angle – Fig. 1). In order to obtain exact scan patterns in our approach we shall utilize a mechanical design program, CATIA V5R20, while we shall maintain

* duma.virgil@osamember.org; phone: +40-751-511451; site: www.3omgroup.appspot.com

Modeling Aspects in Optical Metrology IV, edited by Bernd Bodermann, Karsten Frenner, Richard M. Silver,
Proc. of SPIE Vol. 8789, 878912 · © 2013 SPIE · CCC code: 0277-786X/13/$18 · doi: 10.1117/12.2020386

throughout the study the parameters of the device as they have been defined by Marshall [38]: $k=\theta_2/\theta_1$ and $M=\omega_2/\omega_1$, where ω_1 and ω_2 are the rotating speed of each prism.

This ascertainment of exact scan patterns of Risley prisms scanners, especially using mechanical design programs has not been done yet – to the best of our knowledge. We have completed both the simulations and the experimental validations of these results. Because of space limitations, in this first presentation of our work, a selection of representative modeling and experimental results will be made.

2. SCANNER WITH RISLEY PRISMS

Fig. 1a, b shows one of the configurations of Risley prisms scanners investigated – with the prisms with the vertical facets (perpendicular to the optical axis O.A.) on the exterior of the device. The constructive parameters e – the distance between these facets of the prisms, and L – the distance from the last facet to the screen where the scan patterns will be determined – are pointed out.

Fig. 1c shows the two prisms modeled in CATIA V5R20, as well as the central laser say that is refracted through the prisms. The refraction angles are marked in Fig. 1a, b, where we also noted the total angular deviation D and the linear deviation Δ – for the emergent ray parallel to the incident one and to the O.A. (for the two identical prisms ($\theta_1=\theta_2$) positioned with all the facets parallel). The prisms can be rotated independently with a certain angular increment, and the coordinates of the spot produced by the central ray of the laser beam on the screen are obtained. From these coordinates, the scan patterns can be determined, as it will be presented in the following.

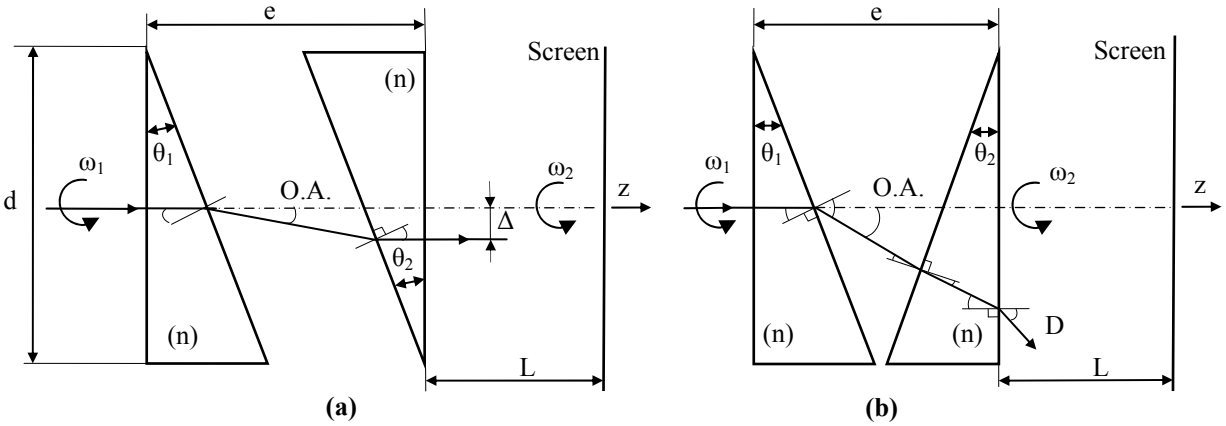

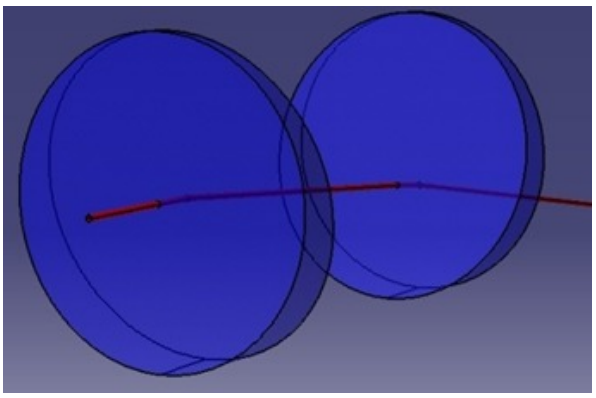

(c)

Figure 1. Optical scanner with Risley prisms – configuration with the plane facets on the exterior: (a), (b) central ray for two positions rotated by 180 degrees of the prisms; (c) modeling of the beam propagation using 3D CATIA.

3. METHOD OF TRACING THE SCAN PATTERNS

Fig. 2 shows a first simulation where one of the prisms is maintained fixed – but in different positions (at 0; 90; 180; 270 degrees) – and the other one is situated completely. The mobile prism will thus produce a circle (in each of the positions of the fixed prism). These circles have equal radiuses and their centers are placed on a circle determined by the incremental movement of the fixed prisms. The differences of the radiuses of the circles of centers and of the radiuses of the circles produced can be noticed – between the two cases.

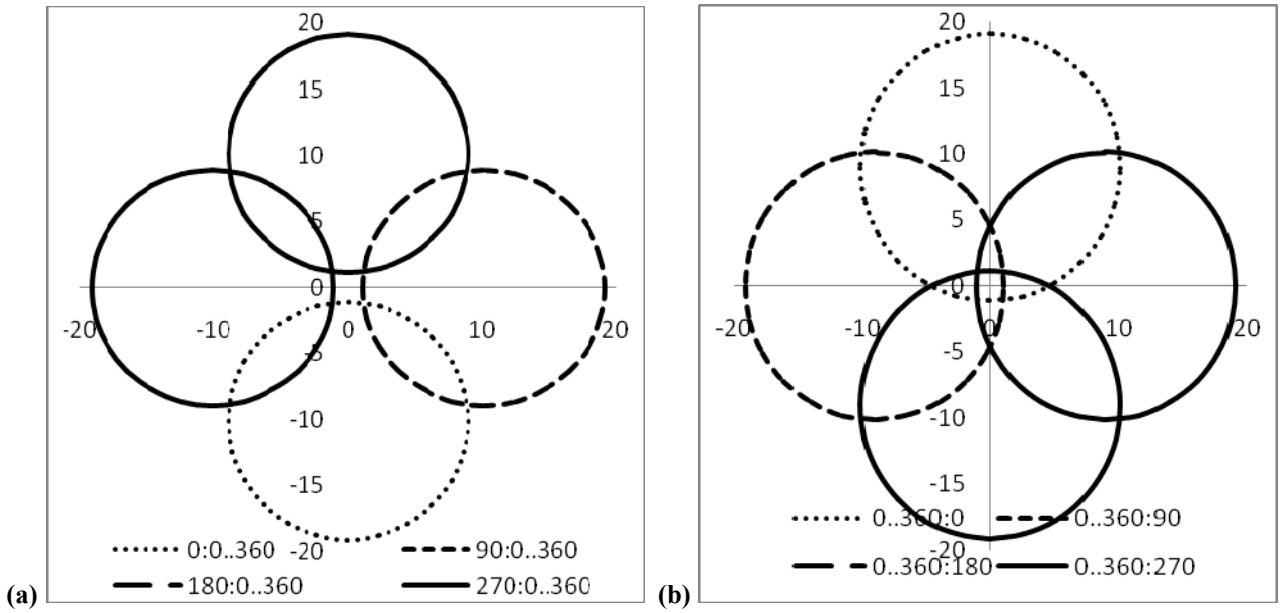

Figure 2. Scan paths produced with two Risley prisms for (a) the first prism fixed at 0; 90; 180; 270 degrees, and the second prism rotational; (b) the first prism rotational, and the second prism fixed at 0; 90; 180; 270 degrees.

Fig. 3 shows the scan patterns produced for a device with identical prisms (k=1), but with different angles θ_1:θ_2 (2:2, 4:4, 6:6, 10:10). Two different situations were considered in Fig. 3a and b: for positive and for negative values of M (equal in module), therefore with the prism rotating in the same sense (a) – with M=4 => ω_2=-4ω_1.

One may notice the differences in shapes between (a) and (b), as the higher relative speed in (b) produces more loops for the pattern. In the same figure (for the same M), the larger scan pattern produced when increasing θ may be remarked – as roughly the maximum deviation angles are approximately proportional to the angles θ of the prisms.

In the following the patterns will be modeled and analyzed, because of space limitations, for one of these two cases, i.e. for M>0. The second case (for M<0) is solved similarly. In Section 5 experimental results will be presented – as examples – for both cases.

4. SCAN PATTERNS FOR M>0

4.1. For k=1 (θ_1=θ_2=2 degrees), the number of loops increases with M (Fig. 4), while for M=1 (ω_1=ω_2), the two prisms rotate together and thus they generate a circle on the screen. The scanning process was simulated by varying the angular speed ω_2 (of Prism 2), and thus obtaining the variation of the trajectory for M=1 to 6.

4.2. By contrast, in the following, in Fig. 5, M was kept constant (M=4) and different pairs of prisms were considered, with the pairs of angles: 2:2, 2:4, 2:6, 2:10, 4:2, 4:4, 4:6, 4:10, 6:2, 6:4, 6:6, 6:10, 10:2, 10:4, 10:6, and 10:10 – therefore with k varying accordingly, from 0.2 to 5.

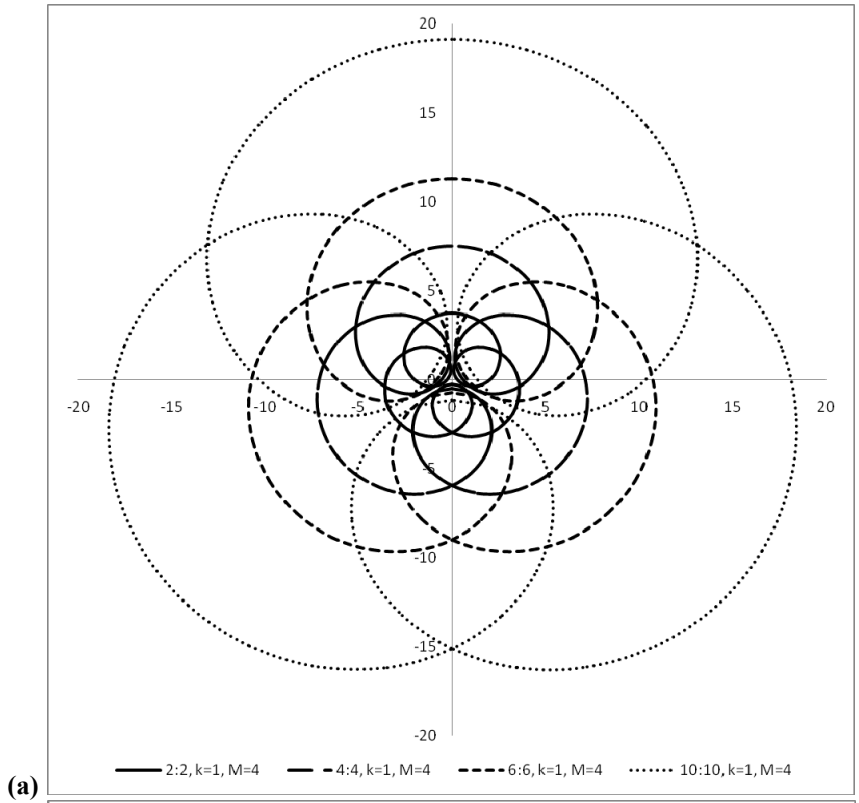

(a)

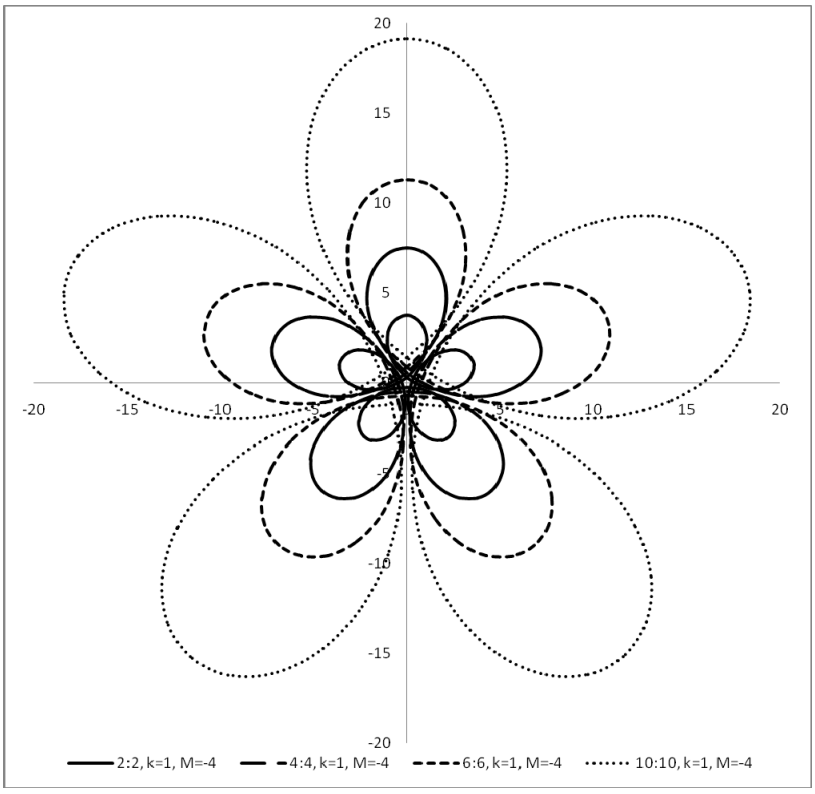

(b)

Figure 3. Scan patterns produced with two rotating Risley prisms for different pairs of identical prisms, with increasing angles (the notation θ_1: θ_2 is used for the angles of a pair of prism that is utilized): (a) $M>0$ (in particular $M=4$); (b) $M<0$ ($M=-4$).

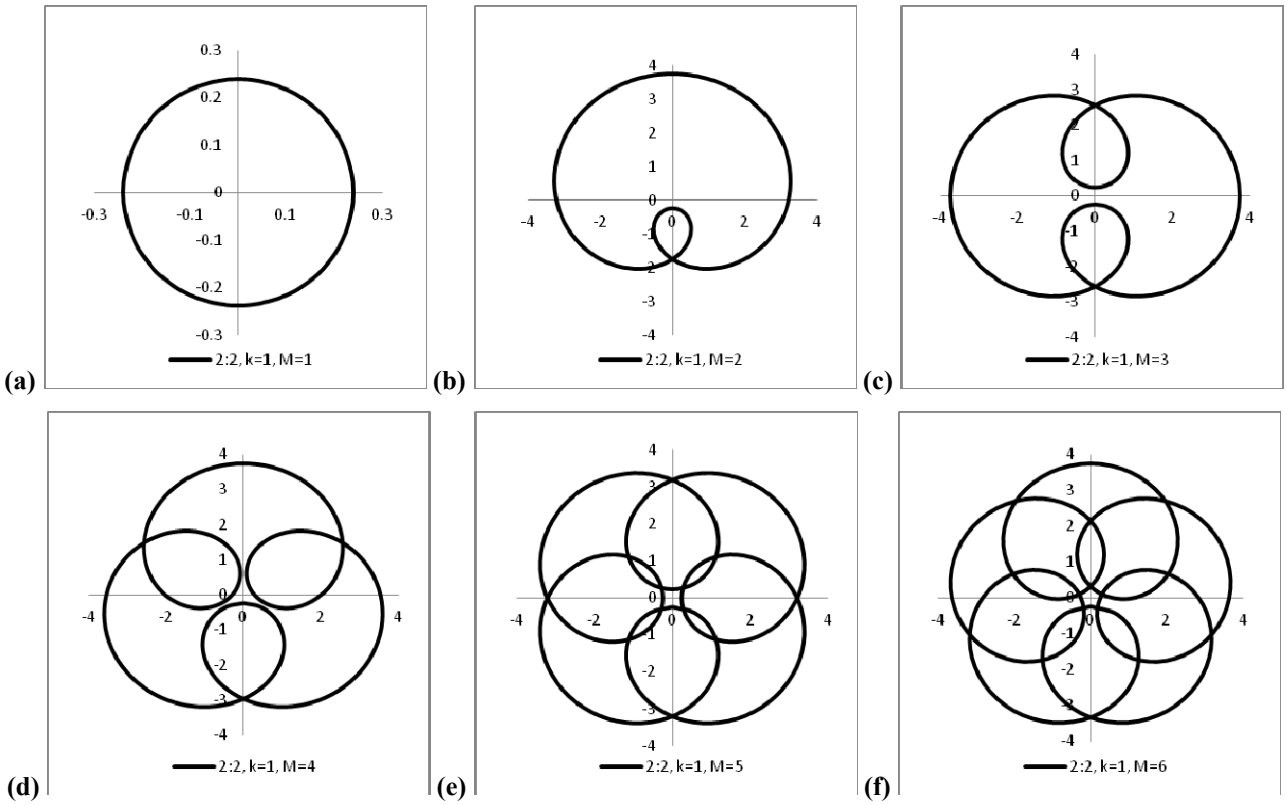

Figure 4. Variation of the scan patterns for the same pair of identical prisms (with the apex of 2 degrees), thus k=1, and for increasing values of the relative rotational speeds of the prisms (therefore of M).

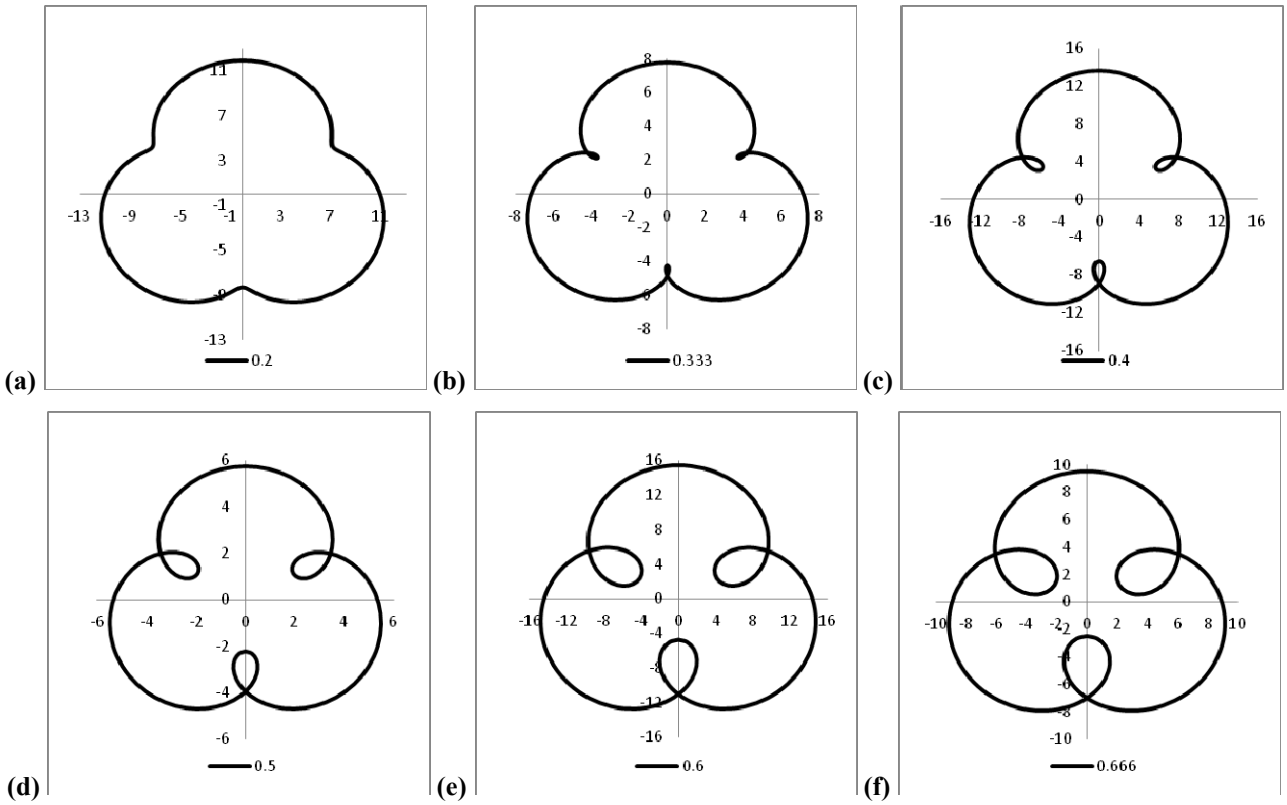

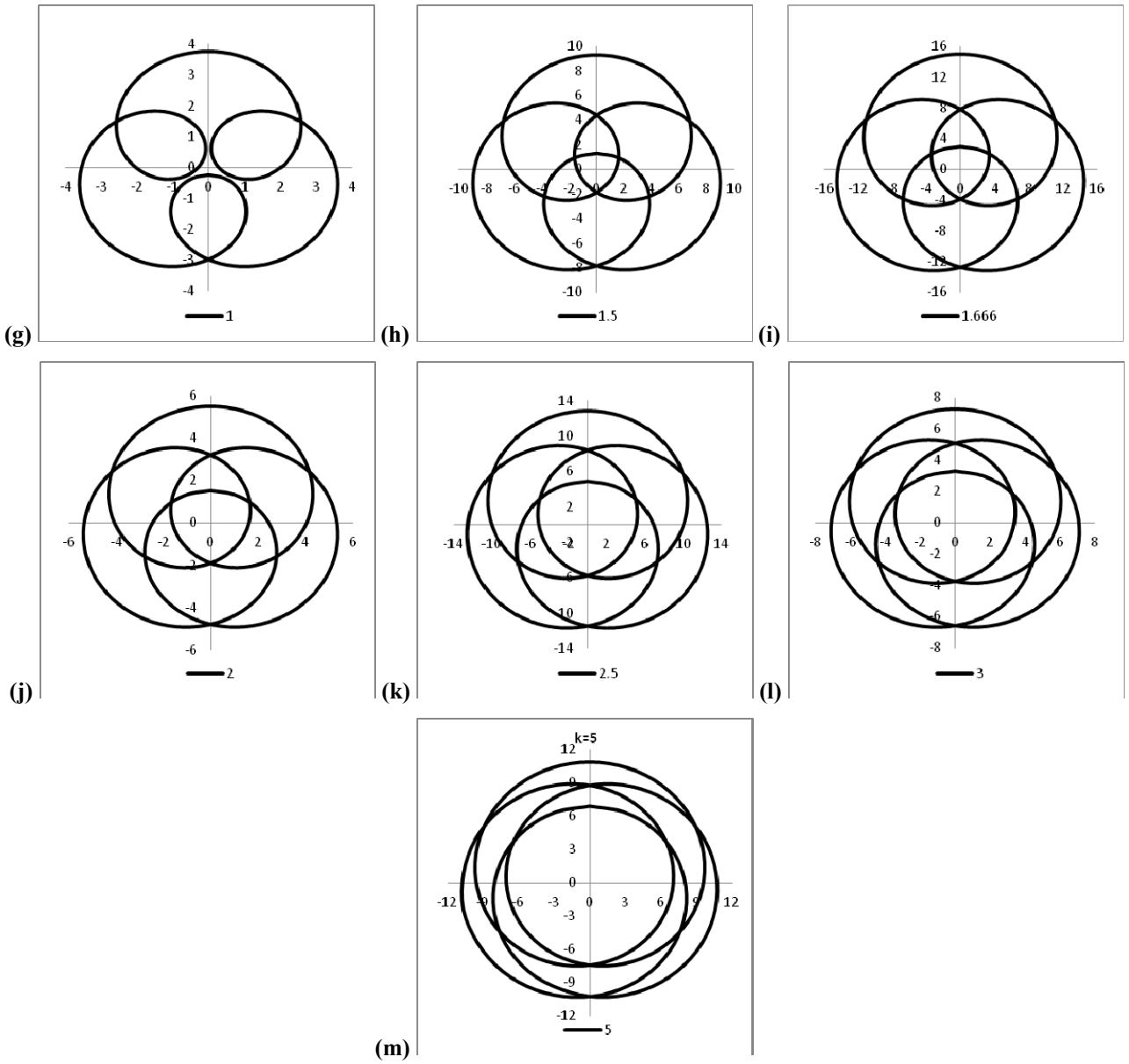

Figure 5. Scan patterns for the same value of M and for an increasing row of values of k.

Several aspects can be concluded: (i) the number of loops increases with k; (ii) the relative dimensions of the loops (with regard to the total dimension of the scanned space) increases; (iii) this dimension of the scanned space is obviously different – it increases with the sum of the angles of the two prisms, $\theta_1+\theta_2$.

4.3. To better compare and conclude on the changes in shape of the scan patterns with the two parameters, k and M, in Fig. 6 a parallel is made between the patterns produced for k=1, 2, 3 and 5 (the pairs of prisms considered are 2:2, 2:4, 2:6, and 2:10) – and at each k, for two values, of M=4 and M=6 of the speed ratio.

One may notice at each M the increase in the outer and inner circle of the scan space – respectively the increase in the radiuses of the circle that inscribed and of the circle that is inscribed in the scan pattern. For the same k, the density of the lines increases with M.

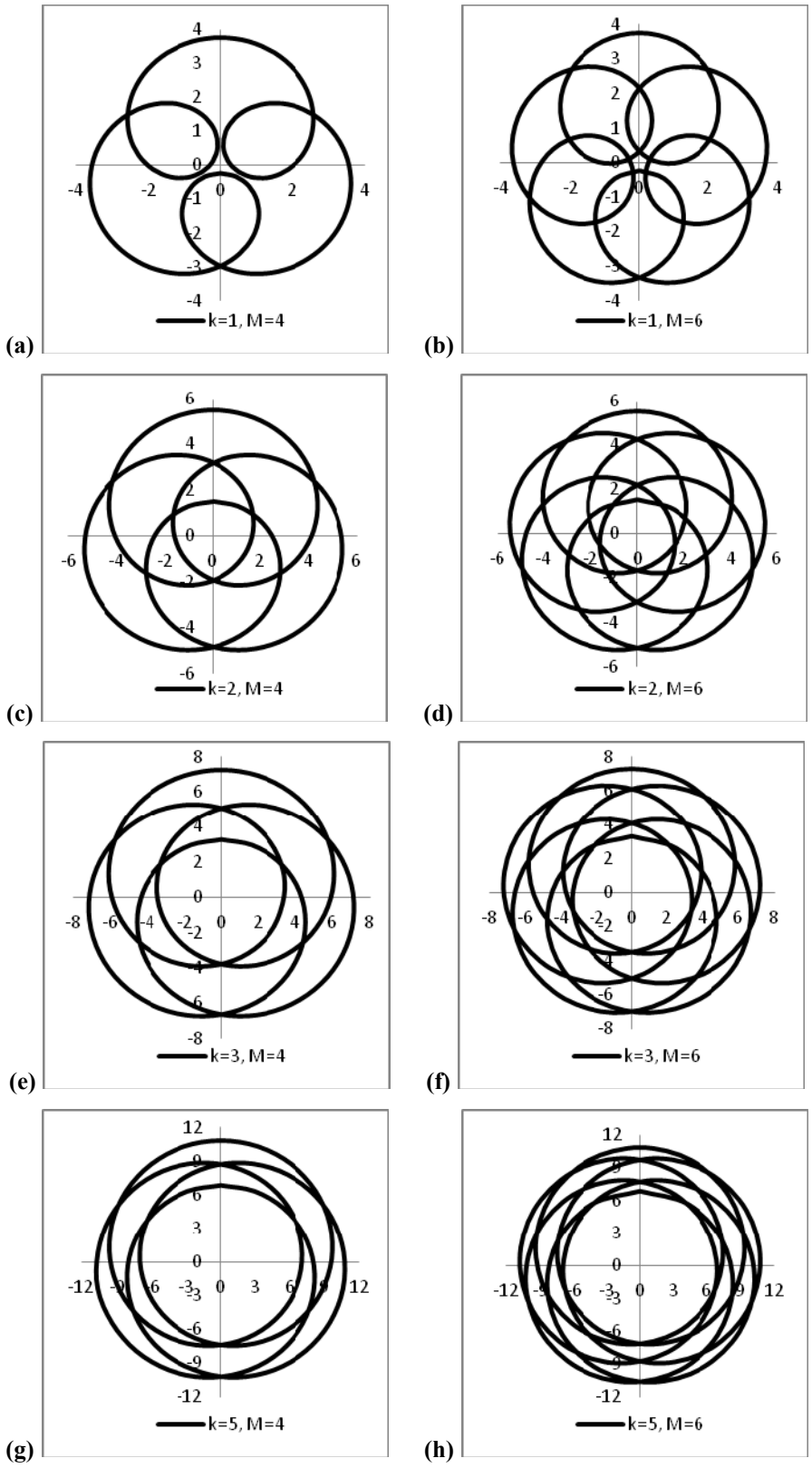

Figure 6. Comparison of the scan patterns produced for increasing k - and for the same k, between two values of M.

4.4. The variation of a scan pattern (obtained for k=1 and for M=6) is presented in Fig. 7 with regard to the distance L to the screen (double in (b) with regard to (a)) and with regard to the distance e between the prisms – Fig. 1a, b (e is double in (c) with regard to (a)). One may notice that with L the scanned space (the radius of the circle that inscribed it) doubles, while the inner "free" space (not scanned) is increased as well.

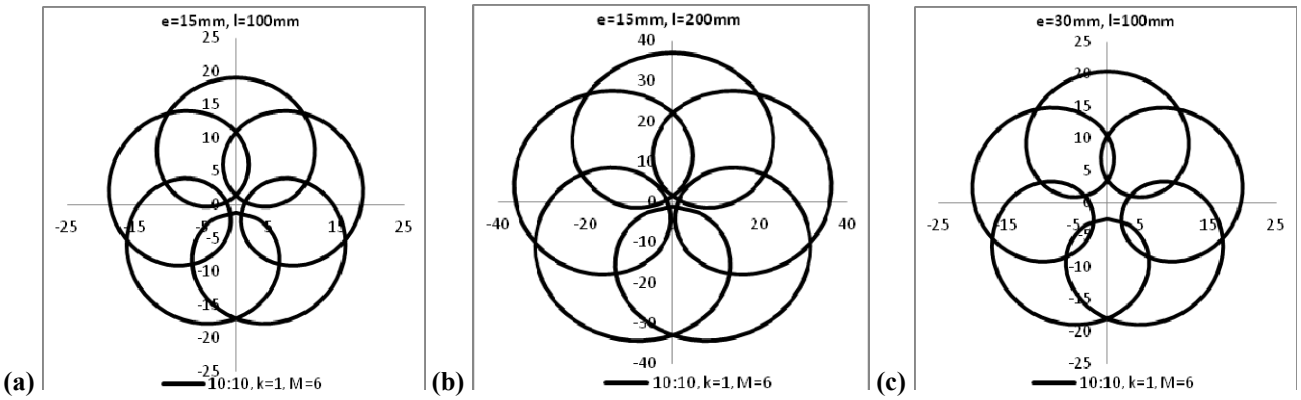

Figure 7. Comparison of the scan patterns produced for the same k and M, but for different values of e and L.

4.5. Combinations between e and L exist to obtain patterns that reach the center (0, 0) of the scanned space, as presented – as an example – in Fig. 8. Actually we have determined that for any k>1 there is a distance L for which such a situation can be obtained. The higher is k, the smaller is this distance L - for which we reach the center (0, 0)) becomes – for the same distance e between the prisms (Fig. 1a, b). For k<1 the trajectory becomes divergent in the center of the pattern (as one may see in Fig. 6a-f), and such a situation – of a trajectory that passes through its center - cannot be reached anymore.

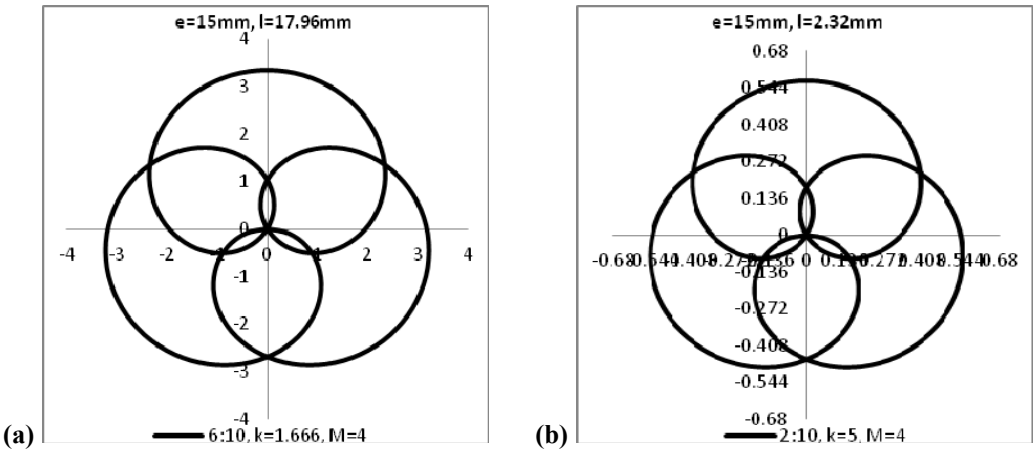

Figure 8. Scan patterns that include the center of the scanned space – for two values of k (M=cst.).

5. SCAN PATTERNS DETERMINED EXPERIMENTALLY

A few examples of patterns determined experimentally with pairs of Risley prisms (Thorlabs™ [38]) for the same k and for the same absolute values of M (but with different signs) are presented in Fig. 9. The experimental results confirm those of the modeling process.

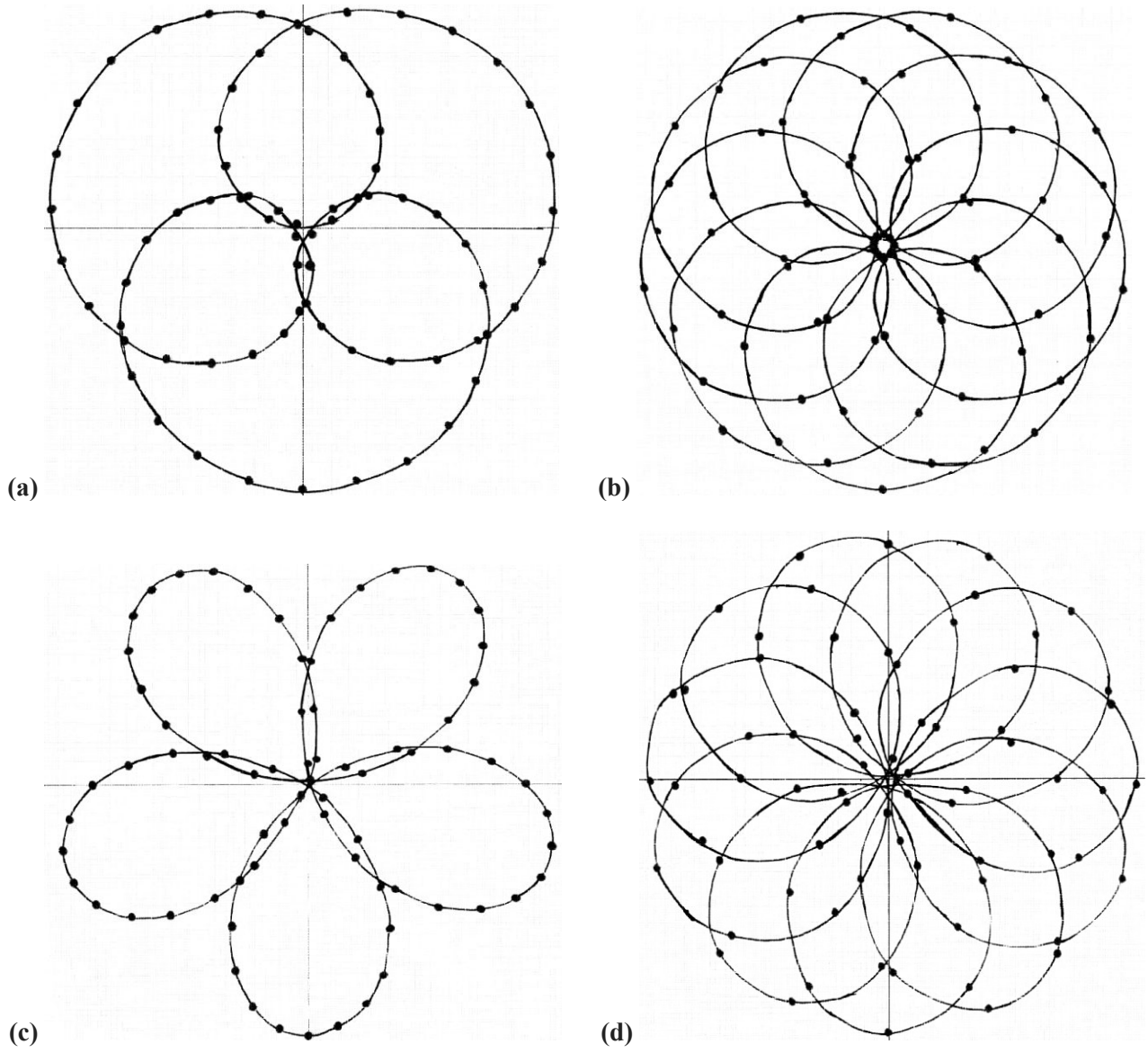

Figure 9. Experimental scan patterns obtained for (a, b) $M>0$: (a) $k=1$, $M=4$; (b) $k=1$, $M=10$, and for (c, d) $M<0$: (a) $k=1$, $M=-4$; (b) $k=1$, $M=-10$.

6. CONCLUSIONS

We have presented some of our results regarding the exact modeling with a mechanical design program, CATIA V5R20, of the scan patterns produced by scanners with rotational Risley prisms. The parameters of the device, in the form they have been introduced by Marshall [38] were utilized: $k=\theta_2/\theta_1$ and $M=\omega_2/\omega_1$. An analysis using these parameters was done in this paper, with a focus on one of the functioning cases, $M>0$, while examples of scan patterns obtained for the other case, for $M<0$, were also presented. Examples of scan patterns obtained experimentally were also presented, as they confirm the results of the modeling process. While we intend to present the entire analysis performed in a future paper, our work will continue with quantifications of these results and with applications of the scanner with Risley prisms in various fields, especially in biomedical imaging, with a focus on OCT, as a possible alternative to generating scan patterns with dual axis galvanometer-based scanners [40].

ACKNOWLEDGEMENTS

This study was supported by a grant of the Romanian National Authority for Scientific Research, CNDI–UEFISCDI project number PN-II-PT-PCCA-2011-3.2-1682.

REFERENCES

[1] Bass, M., Ed., [Handbook of optics], Mc. Graw-Hill Inc., New York, 19.1-19.57 (1995).
[2] Beiser, L., "Fundamental architecture of optical scanning systems," Applied Optics 34, 7307-7317 (1995).
[3] Marshall, G. F., Ed., [Handbook of Optical and Laser Scanning], Marcel Dekker, New York (2004).
[4] Beiser, L., "Design equations for a polygon laser scanner," Proc. SPIE 1454, 60-66 (1991).
[5] Sweeney, M. N., "Polygon scanners revisited," Proc. SPIE 3131, 65-76 (1997).
[6] Montagu, J., „Scanners - galvanometric and resonant," in Encyclopedia of Optical Engineering, R. G. Driggers, C. Hoffman, R. Driggers, Eds., pp. 2465-2487, Taylor & Francis, N.Y. (2003), DOI: 10.1081/E-EOE-120009595.
[7] Kim, K. H., Park, B. H., Maguluri, G. N., Lee, Tom, W., Rogomentich, F. J., Bancu, M. G., Bouma, B. E., de Boer, J. F.; Bernstein, J. J, "Two-axis magnetically-driven MEMS scanning catheter for endoscopic high-speed optical coherence tomography," Opt. Express 15, 18130-18140 (2007).
[8] Duma, V.F., "Contributions to the analysis and the design of scanning systems," Ph.D. Thesis, Polytechnics University of Timisoara (2001).
[9] Duma, V. F., "On-line measurements with optical scanners: metrological aspects," Proc. SPIE 5856, 606-617 (2005).
[10] Duma, V. F., „Novel approaches in the designing of polygon scanners," Proc. SPIE 6785, 6785-1Q (2007).
[11] Duma, V. F., "Optimal Scanning Function of a Galvanometer Scanner for an Increased Duty Cycle," Optical Engineering 49(10), 103001 (2010).
[12] Huang, D., Swanson, E. A., Lin, C. P., Schuman, J. S., Stinson, W. G., Chang, W., Hee, M. R., Flotte, T., Gregory, K., Puliafito, C. A. and Fujimoto, J. G., "Optical coherence tomography," Science 254(5035), 1178-1181 (1991).
[13] Wojtkowski, M., "High-speed optical coherence tomography: basics and applications," Appl. Opt. 49, D30-D61 (2010).
[14] Duma, V. F., Rolland, J. P., and Podoleanu, A. Gh., "Perspectives of optical scanning in OCT," Proc. SPIE 7556, 7556-10 (2010).
[15] Duma, V. F., Lee, K.-S., Meemon, P., and Rolland, J. P., "Experimental investigations of the scanning functions of galvanometer-based scanners with applications in OCT," Appl. Opt. 50, 5735-5749 (2011).
[16] Piyawattanametha, W., Ra, H., Qiu, Z., Friedland, S., Liu, J. T. C., Loewke, K., Kino, G. S., Solgaard, O., Wang, T. D., Mandella, M. J., Contag, C. H., „In vivo near-infrared dual-axis confocal microendoscopy in the human lower gastrointestinal tract." J. Biomed. Opt. 17(2), 021102 (2012).
[17] Li, A., Jiang, X., Sun, J., Bian, Y., Wang, L., Liu, L., "Radial support analysis for large-aperture rotating wedge prism," Optics & Laser Technology 44(6), 1881–1888 (2012).
[18] Warger II, W. C. and DiMarzio, Ch. A., "Dual-wedge scanning confocal reflectance microscope," Opt. Letters 32, 2140-2142 (2007).
[19] Cheng, Y.-S. and Chang, R.-C., „Characteristics of a prism-pair anamorphotic optical system for multiple holography," Opt. Eng. 37, 2717 (1998).
[20] Paez, G., Strojnik, M., and Garcia-Torales, G., "Vectorial shearing interferometer," Appl. Opt. 39, 5172-5178 (2000).
[21] Garcia-Torales, G., Strojnik, M., and Paez, G., "Risley prisms to control wave-front tilt and displacement in a vectorial shearing interferometer," Appl. Opt. 41, 1380-1384 (2002).
[22] Oka, K. and Kaneko, T., "Compact complete imaging polarimeter using birefringent wedge prisms," Opt. Express 11, 1510-1519 (2003).
[23] Zheng, G., Du, C., Zhou, C., Zheng, C., „Laser diode stack beam shaping by reflective two-wedge-angle prism array," Opt. Eng. 44, 044203 (2005).
[24] Kiyokura, T., Ito, T., and Sawada, R., "Small Fourier transform spectroscope using an integrated prism-scanning interferometer," Appl. Spectroscopy 55, 1628-1633 (2001).
[25] Duma, V. F. and Nicolov M., "Neutral density filters with Risley prisms: analysis and design," Appl. Opt. 48, 2678-2685 (2009).

[26] Duma, V. F., "Theoretical approach on optical choppers for top-hat light beam distributions," Journal of Optics A: Pure and Applied Optics 10, 064008 (2008).
[27] Duma, V. F., "Optical choppers with circular-shaped windows: Modulation functions," Communications in Nonlinear Science and Numerical Simulation 16, 2218-2224 (2011).
[28] Duma, V. F., "Prototypes and modulation functions of classical and novel configurations of optical chopper wheels," Latin American Journal of Solids and Structures 10(1), 5-18 (2013).
[29] Tao, X., Cho, H. and Janabi-Sharifi, F., "Active optical system for variable view imaging of micro objects with emphasis on kinematic analysis," Appl. Opt. 47, 4121-4132 (2008).
[30] Tao, X. Cho, H. and Janabi-Sharifi, F., „Optical design of a variable view imaging system with the combination of a telecentric scanner and double wedge prisms," Appl. Opt. 49, 239-246 (2010).
[31] Rosell, F. A., "Prism scanner," J. Opt. Soc. Am. 50, 521 (1960).
[32] Yang, Y., "Analytic solution of free space optical beam steering using Risley prisms," J. Lightwave Technol. 26, 3576-3583 (2008).
[33] Li, Y., "Third-order theory of the Risley-prism-based beam steering system," Appl. Opt. 50, 679-686 (2011).
[34] Li, Y., "Closed form analytical inverse solutions for Risley-prism-based beam steering systems in different configurations," Appl. Opt. 50, 4302-4309 (2011).
[35] Garcia-Torales, G., Flores, J. L., and Muñoz, R. X., "High precision prism scanning system," Proc. SPIE 6422, 64220X (2007).
[36] Li, A., Liu, L. Sun, J., Zhong, X., Wang, L., Liu, D., and Luan, Z., "Research on a scanner for tilting orthogonal double prisms," Appl. Opt. 45, 8063-8069 (2003).
[37] Li, A., Jiang, X., Sun, J., Wang, L., Li, Z., and Liu, L., "Laser coarse–fine coupling scanning method by steering double prisms," Appl. Opt. 51, 356-364 (2012).
[38] Marshall, G. F., "Risley prisms scan patterns," Proc. SPIE 3787, 74-86 (1999).
[39] *Thorlabs Catalog*, Vol. 21 (2011).
[40] Duma, V. F., "Mathematical Functions of a 2-D Scanner with Oscillating Elements," [Modeling, Simulation and Control of Nonlinear Engineering Dynamical Systems], Springer, 243-253 (2009).